Measurements of D^0 production in Zr+Zr and Ru+Ru collisiosns at 200 GeV

Chairperson: Daniel Kikola

Member(s) at large: Guannan Xie

Member for English/Grammar QA: Helen Caines

Member for Code QA: Diptanil Roy

PWG representative: Isaac Mooney

PAs: Yuan Su, Yifei Zhang, Xiaolong Chen

PA representative(s): Yuan Su

July. 31 2024

Outline

- Analytical flow chart of D^0 in Ru+Ru and Zr+Zr collisions
- The physical results shown in the paper draft
- Overall construction and logical flow of the paper draft
- Summary

Analytical flow chart of D^0 in Ru+Ru and Zr+Zr collisions

- **Data sets:** production_isobar_2018
- **Production tag:** P20ic
- **Trigger:** 600001, 600011, 600021, 600031 (MB)
- **Embedding Request ID:** 20201503
- **Badrunlist:** Ru+Ru Zr+Zr (50+35)

Analysis cuts

Main event Level cuts	
Cuts	Value
$\|V_z\|$	(-35,25) cm
V_r	< 2. cm
VzDiff	< 3. cm
0-80%	

Main track quality cuts	
Cuts	Value
p_T (GeV/c)	> 0.6
TPC Nhits	⩾20
nHits/HitsMax	[0.52, 1.2]
gDCA	⩽ 2.0 cm

PID cuts	
Cuts	Value
p < 1.6 && β > 0	hybrid PID functions
p ≥ 1.6 && β > 0 (Pion)	hybrid PID functions

D^0 reconstruction

Γ_i/Γ ~ 3.95%

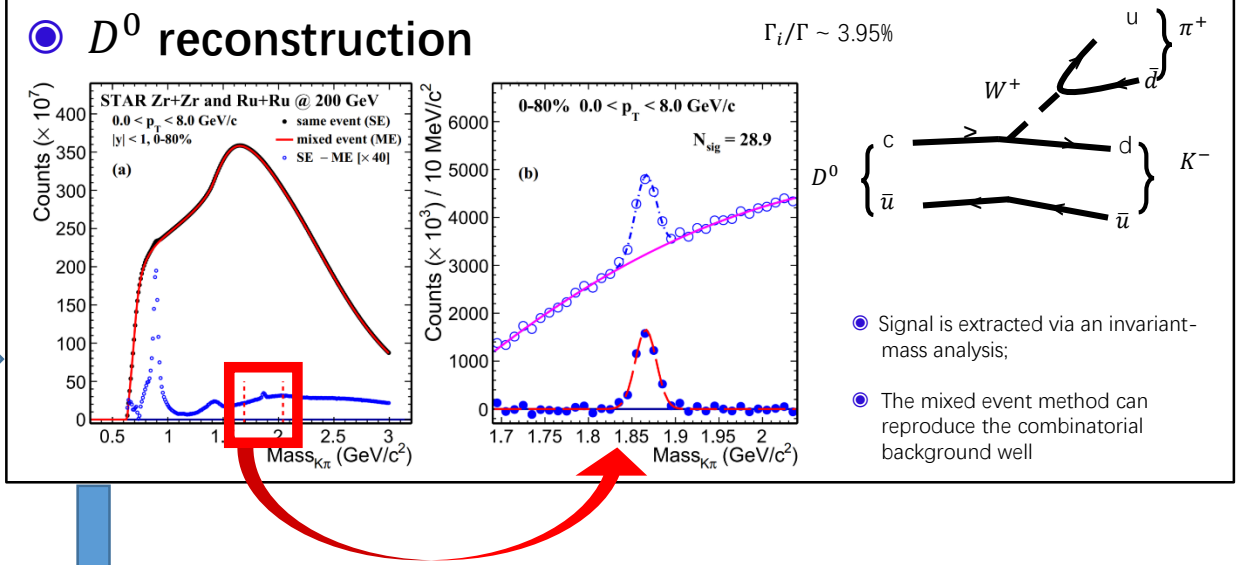

- Signal is extracted via an invariant-mass analysis;
- The mixed event method can reproduce the combinatorial background well

Efficiency correction & Systematic uncertainties

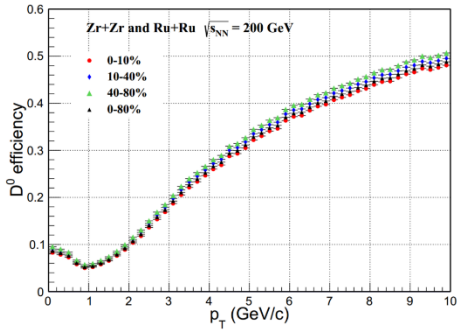

Fig. 4 D^0 efficiency as a function of D^0 transverse momentum at 0–10%, 10–40%, 40–80% and 0–80% centrality classes.

Table 2 Systematic uncertainties in D^0 analysis

		0–10%	10–40%	40–80%
spectra	Raw yield	3.9-16.5%	3.7-10.5%	4.0-8.5 %
	Double counting	0.7%	0.8%	0.9%
	Track p_T variation	10.6%	9.3%	7.3%
	ϵ_{PID}	3%	3%	3%
	TRE	2-6%	2-6%	2-6%
	BR	0.5%	0.5%	0.5%
R_{AA}	$\langle N_{bin} \rangle$	1.6%	0.6%	0.4%
	pp base	20.6-71.8%	20.6-71.8%	20.6-71.8%
		0–10%		10–40%
Rcp (/40–80%)	Raw yield	13.6-20.7%		12.4-16.5 %
	TRE	0		0
	BR	0		0
Integrated cross section		$p_T > 0$		$p_T > 4$ GeV/c
	Total	12.7-15.8%		12.0-15.2 %

The physical results shown in the paper draft

D^0 production in Zr+Zr and Ru+Ru collisions

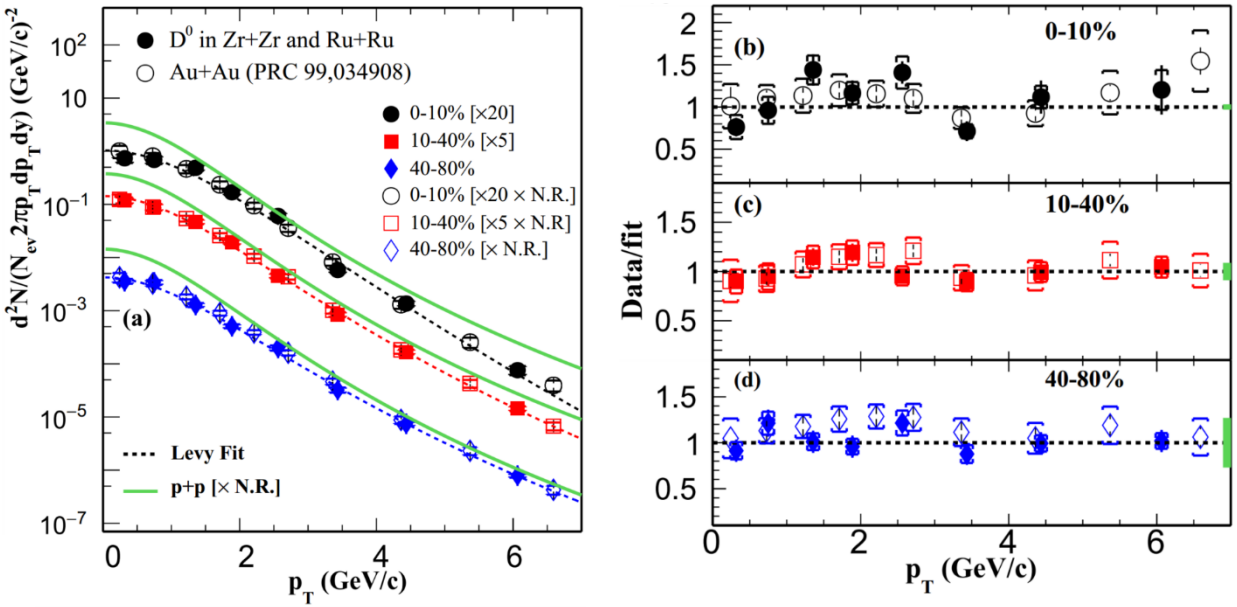

Fig. 5 D^0 invariant yields at mid-rapidity ($|y| < 1$) as a function of p_T for different centrality classes in Ru+Ru and Zr+Zr collisions compared to that of D^0 in Au + Au collisions at the same energy (a). Vertical lines and square brackets on data points indicate statistical and systematic uncertainties, respectively. The Data/fit results are shown in the bottom panels (b), (c), and (d), where the fits are applied on corresponding D^0 p_T spectra in Ru+Ru and Zr+Zr collisions by a Levy function.

- charm quarks may have undergone a similar dynamic process

D^0 thermal properties (BW, TBW, m_T spectra)

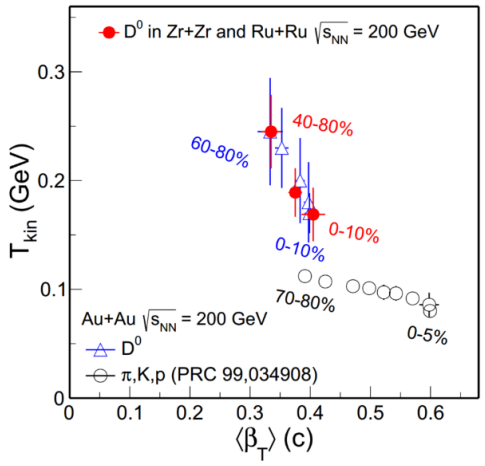

Fig. 7 The correlation between T_{kin} and $\langle\beta_T\rangle$, extracted from the Blast-wave fits for different hadron p_T spectra

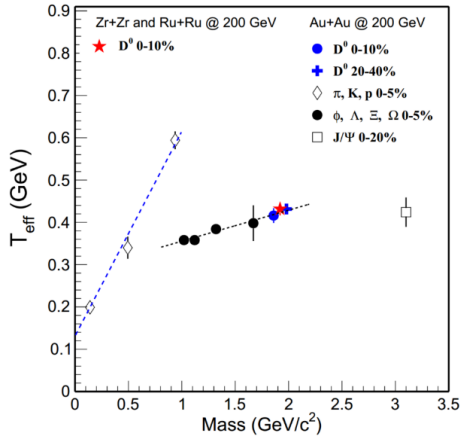

Fig. 9 T_{eff} obtained from m_T spectra fits as a function of the hadron mass in isobar and Au + Au collisions.

Table 3 Tsallis blast-wave model fits parameters to D^0 p_T-differential spectra in Ru+Ru and Zr+Zr collisions.

Centrality	$\langle\beta_T\rangle$(c)	$q-1$
0-10%	0.282±0.018	0.070±0.007
10-40%	0.207±0.030	0.080±0.007
40–80%	0.189±0.031	0.089±0.005

- D^0 invariant yield at mid − rapidity (|y|<1) vs. p_T for different centrality bins fitted with blast-wave function.
- D^0 freeze out temperature in Isobar collisions are consistent with that of in Au + Au collisions for the same centrality.
- The average flow velocity increases with central collision, and (q −1) is also found to be close to zero.

The physical results shown in the paper draft

- D^0 R_{AA} & R_{CP} in Zr+Zr and Ru+Ru collisions

- D^0 R_{AA} for different centrality classes in Isobar collisions compared to that of Au + Au results, quenching of hard probes.

- R_{CP} vs. p_T, D^0 production in central collisions show a suppression behavior w.r.t mid-central collisions.

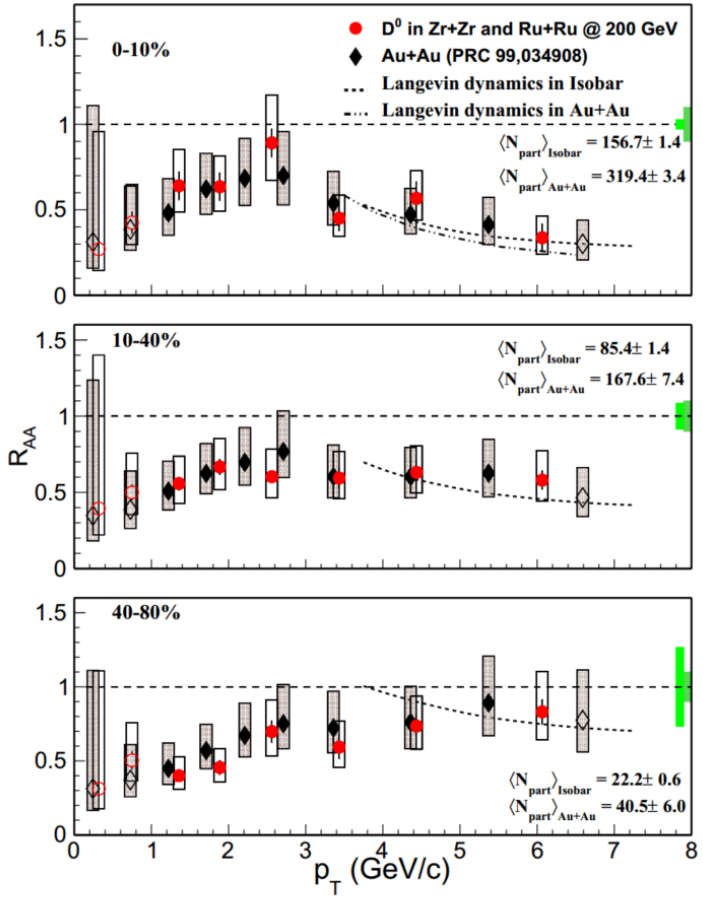

Fig. 10 D^0 R_{AA} within the same centrality are compared between isobar and Au+Au collisions. The dashed lines are model curves based on Langevin dynamics.

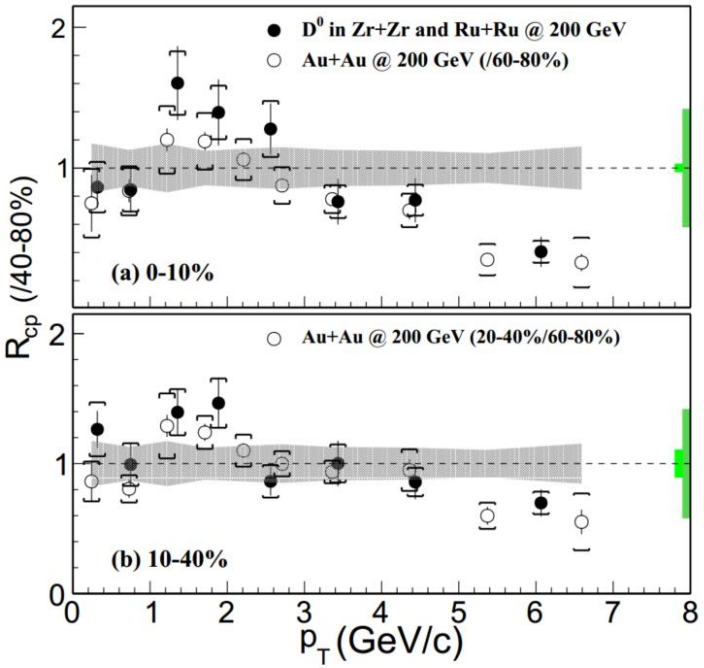

Fig. 13 D^0 R_{CP} with the 40–80% spectrum as the reference for 0–10% (a) and 10–40% (b) in Ru+Ru and Zr+Zr collisions at $\sqrt{s_{NN}}$ = 200 GeV compared to corresponding results in Au + Au collisions at the same center-of-mass energy [3]. The statistical and systematic uncertainties are shown as error bars and brackets on the data points. The grey bands around unity and boxes on the right depict uncertainty in Au + Au collisions.

The physical results shown in the paper draft

- D^0 R_{AA} & R_{CP} in Zr+Zr and Ru+Ru collisions

- D^0 integrated R_{AA} vs. $< N_{part} >$ for p_T > 0 and p_T > 4 GeV/c in Isobar and Au + Au collisions.

- D^0 R_{AA} vs. p_T with similar $< N_{part} >$ between different system, no obvious colliding system dependence is observed, and higher precision is needed to draw the differences between the dependencies with respect to centrality and $< N_{part} >$

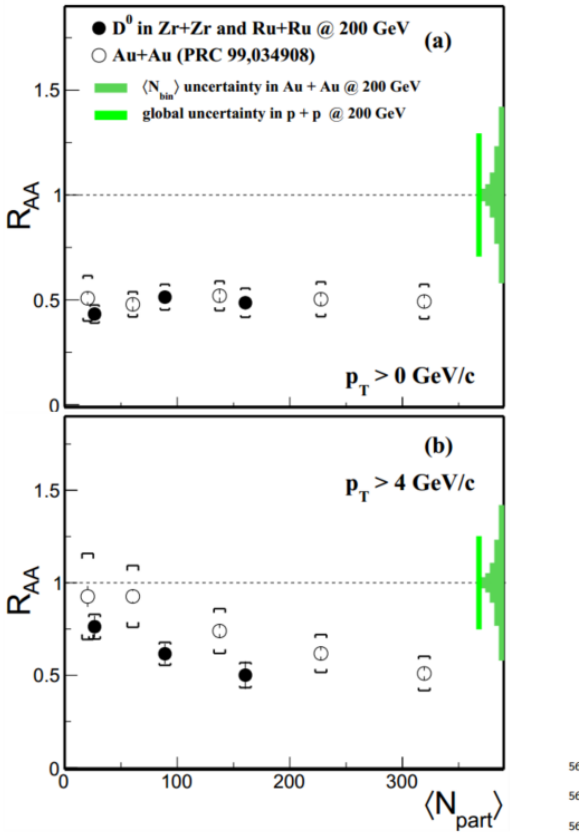

Fig. 12 D^0 R_{AA} as a function of $\langle \mathrm{N_{part}} \rangle$ for $p_{\mathrm{T}} > 0$ (a) and $p_{\mathrm{T}} > 4$ GeV/c (b). The light and dark green boxes on the right depict the global uncertainty in pp collisions and the normalization uncertainties of the $\langle N_{bin} \rangle$ in Au + Au collisions, respectively. The dark green boxes from left to right correspond to central to peripheral collisions.

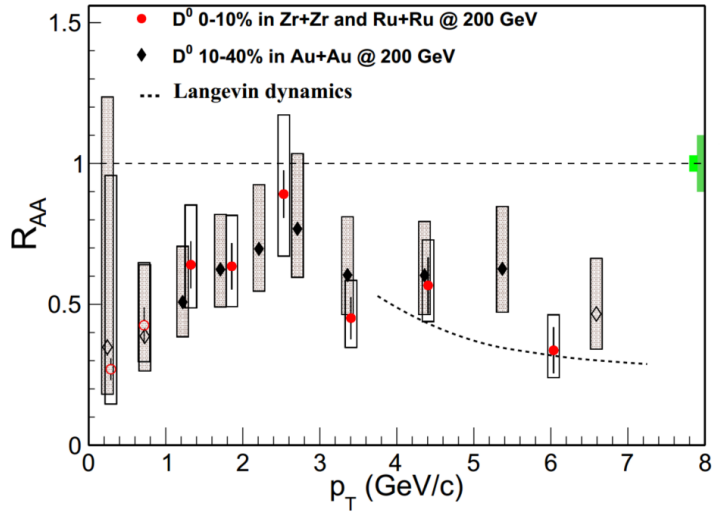

Fig. 11 D^0 R_{AA} in central Ru+Ru and Zr+Zr collisions compared to that in semi-central Au + Au collisions, which has a similar $\langle \mathrm{N_{part}} \rangle$.

Overall construction and logical flow of the paper draft

- **Introduction:** background & motivation & definition $R_{AA} = \frac{\sigma_{inel}^{NN} d^2 N_{AA}^{D^0}/dp_T dy}{< N_{coll} > d^2\sigma_{pp}^{D^0}/dp_T dy}$
- **Data set and experimental apparatus:** mainly detector parameter (TPC & TOF) in this analysis
- **Data analysis :**
  - D^0-meson reconstruction
  - D^0 p_T spectra correction
  - Systematic uncertainties
- **Results and discussion:**
  - N_{bin} scaling of D^0 production cross section
  - Bulk properties
  - nuclear modifcation factor - R_{AA} and R_{CP}
- **Summary**

The TPC, which is used to detect charged particles has a pseudorapidity range of $|\eta| < 1$ with full 2π azimuthal coverage and a transverse momentum (p_T) lower limit of 0.2 GeV/c, is based on a cylindrical gaseous chamber with longitudinal and radial dimensions of $|z| <$ 210 cm and $50 < r < 200$ cm, respectively. The primary vertex with a radial distance (V_r) and the vertex position along the beam direction (V_z) in each collision is also reconstructed by TPC, $V_r < 2$ cm and $-35 < V_z <$ 25 cm are required in this analysis.

A full-barrel TOF is a large-area cylindrical array made of multigap resistive plate chambers and built outside the TPC. It covers the full azimuthal angle (0-2π) with the pseudorapidity region $|\eta| < 1$. The time-of-flight with an approximate time resolution of 100 ps is measured as the difference between the start time given by the VPD and the stop time measured by the TOF.

Summary

- D^0-meson productions are **firstly measured** at mid-rapidity (|y| < 1) in 200 GeV isobar collisions。
- The number of binary collisions **scale effect of D^0** production cross section between isobar and Au + Au collisions is observed。
- The strong suppression of D^0 nuclear modification factor R_{AA} is observed for p_T > 3 GeV/c in central isobar collisions, demonstrating that **charm quarks suffer significant energy loss** in the QGP.
- No significant systematic dependence of D^0 kinetic freeze-out properties in central collisions between isobar and Au + Au collisions within uncertainties is observed.

Backup

Analysis details